Parametric Reduced-Order Models of Battery Pack Vibration Including Structural Variation and Pre-stress Effects

Sung-Kwon Hong[(1)], Bogdan I. Epureanu[(1)], Matthew P. Castanier[(2)]
(1) University of Michigan, (2) US Army RDECOM-TARDEC

ABSTRACT

The goal of this work is to develop an efficient numerical modeling method for the vibration of hybrid electric vehicle (HEV) battery packs to support probabilistic forced response simulations and fatigue life predictions. There are two important sources of variations in HEV battery packs that affect their structural dynamic response. One source is the uncertain level of pre-stress due to bolts or welds used for joining cells within a pack. The other source is small structural variations among the cells of a battery pack. The structural dynamics of HEV battery packs are known to feature very high modal density in many frequency bands. That is because packs are composed of nominally identical cells. The high modal density combined with small, random structural variations among the cells can lead to drastic variations in the dynamic response compared with those of the ideal nominal system. Therefore, it is important to perform probabilistic simulations of the structural response with pre-stress variations and cell-to-cell parameter variations in order to accurately predict the fatigue life of a pack. In this paper, a new parametric reduced-order model (PROM) formulation is derived for HEV battery pack vibration by employing several key observation; namely (1) the stiffness matrix can be parameterized for different levels of pre-stress, (2) the mode shapes of a battery pack with cell-to-cell variation can be represented as a linear combination of the mode shapes of the nominal system, and (3) the frame holding each cell has vibratory motion. These key observations are exploited to include the effects of pre-stress and cell-to-cell variations directly in the PROM formulation. A numerical example of an academic battery pack with pouch cells is presented to demonstrate that the PROMs capture the effects of both pre-stress and structural variation on HEV battery packs. The PROMs are validated numerically by comparing their forced response predictions with those from full-order finite element models (FEMs) of the same systems.

INTRODUCTION

Typical hybrid electric vehicle (HEV) battery packs are assembled by bolts or welds for joining cells within the pack and for integrating the battery structure into the rest of the vehicle. The pre-stress due to joining can affect the dynamic response of the structures significantly. Additionally, the battery pack structure includes 100–300 cells. Because these cells are nominally identical, battery packs fall under the class of structures known as periodic structures. The dynamics of periodic structures are known to feature very high modal density in many frequency bands. The high modal density combined with small, random structural variations among the cells (which are unavoidable in practice) can lead to drastic consequences on the structural dynamics. Therefore, it may be important to use statistical dynamic response calculations for predicting the fatigue life of a pack, especially for a pack with pouch cells. Such statistical calculations are hard to perform using linear methods because the mode shapes of a pack depend in a nonlinear fashion on the parameters of each cell. The alternative is to use sample-based statistical analyses. However, typical finite element models (FEMs) of battery packs have several million degrees of freedom (DOFs). Thus, the computational time for obtaining just a single sample can be on the order of a day.

To overcome this issue, in the field of structural dynamic analysis, component mode synthesis (CMS) [1-7] is well established as an alternative to conventional FEMs with large numbers of DOFs. CMS belongs to a wide class of domain decomposition techniques. CMS divides the global structure into several substructures, and the DOFs of each individual substructure are reduced significantly. Then, the substructures are reconnected, and the dynamic response of the system is predicted very efficiently and accurately. However, classical CMS must be modified in order to account for parametric variability in the structure. Thus, alternate, design-oriented techniques have been developed. One such approach is to generate what is referred to as parametric reduced-order models (PROMs). PROMs were introduced initially by Balmès [8-9] to avoid the expensive process of reanalysis of complex structures. In addition, several other PROM methods have been developed [10-14]. In particular, the multiple-component PROMs (MC-PROMs) [13] have been developed by the authors. MC-PROMs are well suited for the structure modeled with shell-type finite elements. However, MC-PROMs have several drawbacks, namely: (1) a numerical

Report Documentation Page

Form Approved
OMB No. 0704-0188

1. REPORT DATE	2. REPORT TYPE	3. DATES COVERED
19 NOV 2012	**Journal Article**	**10-03-2012 to 18-10-2012**

4. TITLE AND SUBTITLE	5a. CONTRACT NUMBER
Parametric Reduced-Order Models of Battery Pack Vibration Including Structural Variation and Pre-stress Effects	**W56H2V-04-2-0001**
	5b. GRANT NUMBER
	5c. PROGRAM ELEMENT NUMBER
6. AUTHOR(S)	5d. PROJECT NUMBER
Sung-Kwon Hong; Bogdan Epureanu; Matthew Castanier	5e. TASK NUMBER
	5f. WORK UNIT NUMBER
7. PERFORMING ORGANIZATION NAME(S) AND ADDRESS(ES)	8. PERFORMING ORGANIZATION REPORT NUMBER
University of Michigan,4260 Plymouth Road,Ann Arbor,Mi,48109	**; #23505**
9. SPONSORING/MONITORING AGENCY NAME(S) AND ADDRESS(ES)	10. SPONSOR/MONITOR'S ACRONYM(S)
U.S. Army TARDEC, 6501 East Eleven Mile Rd, Warren, Mi, 48397-5000	**TARDEC**
	11. SPONSOR/MONITOR'S REPORT NUMBER(S)
	#23505

12. DISTRIBUTION/AVAILABILITY STATEMENT

Approved for public release; distribution unlimited

13. SUPPLEMENTARY NOTES

14. ABSTRACT

The goal of this work is to develop an efficient numerical modeling method for the vibration of hybrid electric vehicle (HEV) battery packs to support probabilistic forced response simulations and fatigue life predictions. There are two important sources of variations in HEV battery packs that affect their structural dynamic response. One source is the uncertain level of pre-stress due to bolts or welds used for joining cells within a pack. The other source is small structural variations among the cells of a battery pack. The structural dynamics of HEV battery packs are known to feature very high modal density in many frequency bands. That is because packs are composed of nominally identical cells. The high modal density combined with small, random structural variations among the cells can lead to drastic variations in the dynamic response compared with those of the ideal nominal system. Therefore, it is important to perform probabilistic simulations of the structural response with pre-stress variations and cell-to-cell parameter variations in order to accurately predict the fatigue life of a pack. In this paper, a new parametric reduced-order model (PROM) formulation is derived for HEV battery pack vibration by employing several key observation; namely (1) the stiffness matrix can be parameterized for different levels of pre-stress, (2) the mode shapes of a battery pack with cell-to-cell variation can be represented as a linear combination of the mode shapes of the nominal system, and (3) the frame holding each cell has vibratory motion. These key observations are exploited to include the effects of pre-stress and cell-to-cell variations directly in the PROM formulation. A numerical example of an academic battery pack with pouch cells is presented to demonstrate that the PROMs capture the effects of both pre-stress and structural variation on HEV battery packs. The PROMs are validated numerically by comparing their forced response predictions with those from full-order finite element models (FEMs) of the same systems.

15. SUBJECT TERMS					
16. SECURITY CLASSIFICATION OF:			17. LIMITATION OF ABSTRACT	18. NUMBER OF PAGES	19a. NAME OF RESPONSIBLE PERSON
a. REPORT **unclassified**	b. ABSTRACT **unclassified**	c. THIS PAGE **unclassified**	**Public Release**	**11**	

Standard Form 298 (Rev. 8-98)
Prescribed by ANSI Std Z39-18

instability of system level matrices can be encountered due to the transformation matrix, (2) MC-PROMs do not capture well elemental level nonlinearities for thickness variations of brick type finite elements, and (3) the interface DOFs are hard to reduce. Thus, the next-generation PROM (NX-PROM) technique has been developed recently to overcome these drawbacks [14]. The concepts used in NX-PROMs are applied herein to capture the pre-stress variations.

The PROM techniques are highly efficient methods for estimating the statistics of the structural dynamic response. However, for a structure with very high modal density, previously developed PROMs have to be modified to efficiently capture the dynamic response. In particular, such a modification can be similar to the component mode mistuning (CMM) [15] method. CMM was developed for predicting the dynamic response of bladed disks found in turbo-machinery. Typically, these bladed disks suffer from high modal density. Thus, small structural variations in the blades significantly affect the system-level dynamic response. Nonetheless, it has been shown that the mode shapes of a mistuned bladed disk can be represented as a linear combination of the mode shapes of the tuned bladed disk [16]. This allows CMM to capture the dynamic response effectively with a small number of DOFs, and that is the inspiration for the new PROMs introduced in this work.

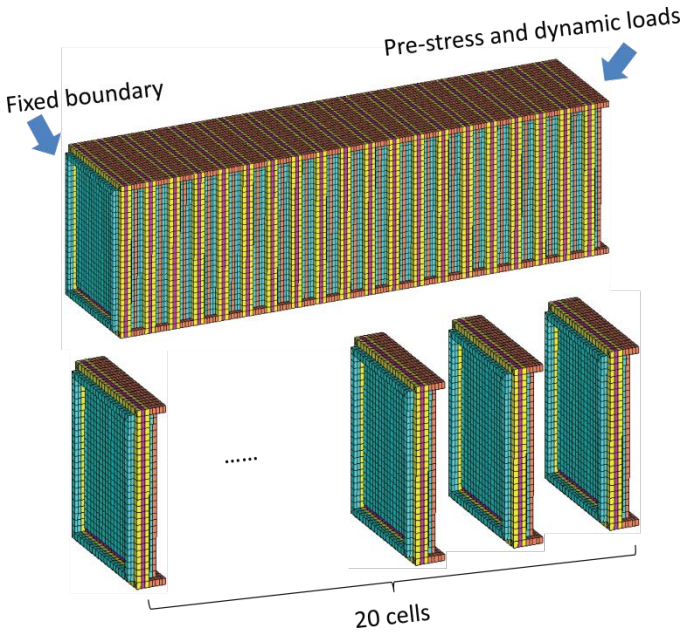

Figure 1. The geometry of a battery pack with 20 pouch cells

The focus of this work is to predict the vibratory response of a battery pack which may suffer from vibration localization. Localization can lead to damage because of excessive vibrations and stress levels, which in turn can lead to mechanical or electromechanical failure. Localization depends on small variations in structural properties from cell to cell. Those variations are random. Hence, a statistical characterization of the dynamics of the pack is necessary. Thus, the work focuses on predicting the probability that a given cell experiences larger amplitudes than for the nominal case (when all variabilities are absent). The probability that a cell mechanically or electromechanically fails is related to the probability that a cell experiences larger vibrations. The vibration response is characterized in this work as typically done in vibration analyses, namely by using the complex displacement amplitudes throughout the system. The new method, however, is much faster (e.g., 10,000 times faster as shown in this paper). For studies of mechanical fatigue, the spatial derivatives (gradients) of these displacements can be used to obtain the corresponding stresses. This approach, which is sometimes referred to as stress recovery, is a standard analysis procedure with a relatively low computational cost. It is often available in finite element packages for structural dynamics, and it has also been implemented directly in reduced-order modeling methods [17].

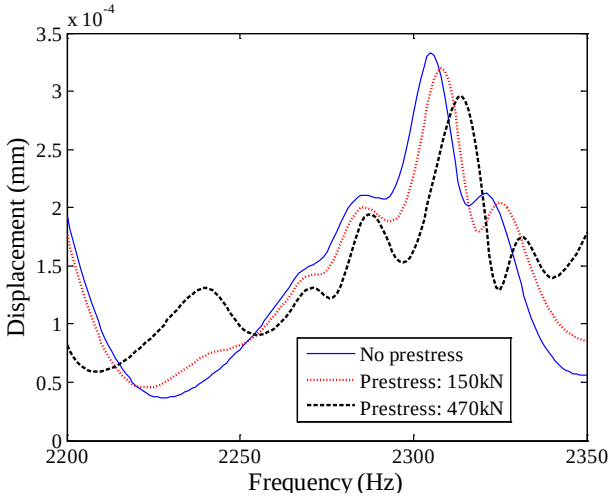

Figure 2. Forced response of the center node of the 1st cell for different levels of pre-stress without structural variation

STRUCTURAL PROPERTIES AND DYNAMIC CHARACTERISTICS OF BATTERY PACKS

HEV battery packs typically have 100 – 300 individual cells that are nominally identical. To demonstrate the structural dynamic characteristics of a battery pack, a simplified academic model of a pack of pouch cells was developed using finite elements as shown in Figure 1. The nodes on one end of the pack are totally fixed. The pre-stress and dynamic loads are applied to nodes on the other end of the structure. The pre-stress loads are applied to the longitudinal direction to compress the structure, and the harmonic excitations are applied to all three (x, y, z) directions. The excitation frequencies are in the range of 2,200 – 2,350Hz. A total of 20 nominally identical cells are stacked. Typically, foam or epoxy stiffness layers can be placed between cells. These

elements are nonlinear materials, but they are soft. Thus, herein we ignore these nonlinear materials.

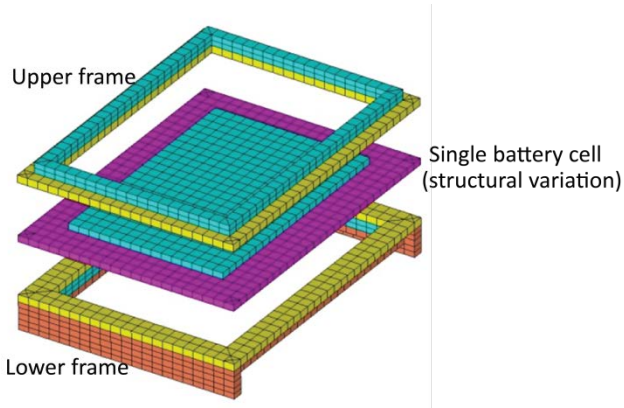

Figure 3. The geometry of a single pouch cell

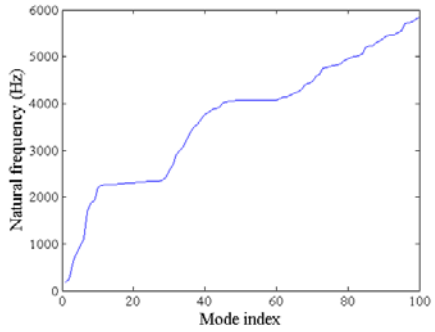

Figure 4. Natural frequencies of the academic battery pack without pre-stress and without cell-to-cell variations

To evaluate how the pre-stress variations in the structure affect the structural response, we applied two different levels of pre-stress, which are 150kN and 470kN. Figure 2 shows the forced responses of the center node of the 1st cell for the different levels of pre-stress. The responses obtained by full-order models are significantly different for each level of pre-stress.

Table 1. Two cases of Young's modulus variations

Case 1		Case 2	
Cell	Variation	Cell	Variation
1	+5%	3	+3%
5	-7%	9	-5%
12	+1%	13	+2%
16	+3%	20	-5%

Figure 3 shows a single cell and the frames that join it to the adjacent cells. The single pouch cell is a plate-like structure for which the small, random structural variations are modeled by perturbations to the elastic modulus (E). The (nominally identical) cells are mechanically coupled through the frames, which induces a high modal density to the entire battery pack structure, as shown in Figure 4. The flat regions in Figure 4 indicate frequency ranges of high modal density. For example, there are over 20 modes in the range 2,200 – 2,300Hz. If the battery pack had more cells, the modal density would be even higher.

To examine how structural variations in the cells affect the structural response, we applied the elastic modulus variations described in Table 1, and compared the mode shapes of the structure with nominal parameters (no variation) and the mode shapes of the structure for cases 1 and 2. These mode shapes are shown in Figure 5. To observe the consequences of small parameter variations, cases 1 and 2 only had variations in 4 cells. In general, all cells have some variability.

Although the structural variations are small, the mode shapes are affected significantly. In particular, note that some mode shapes are localized at a few cells in which there are no parameter variations.

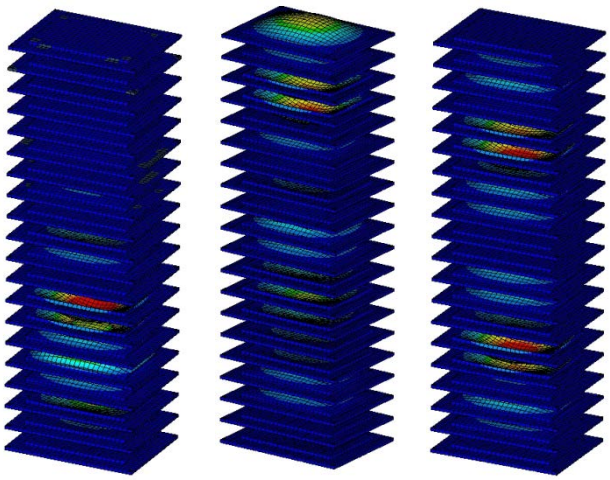

Figure 5. Mode shapes of the nominal structure with identical cells (left) and the structures with cases 1(center) and 2 (right) of cell parameter variations

Forced responses were compared for each case of variation also, as shown in Figure 6. These results show that small local structural variations can induce large changes in the global response.

Figure 6 shows the response of the 4th cell (top plot) and the 6th cell (bottom plot). As shown in Table 1, there are no variations in the parameters of cells 4 and 6. However, there are significant changes in the dynamic response of these cells. For example, the maximum response of the 6th cell of the battery with nominal parameters is approximately 0.0085mm, whereas the maximum response of the same cell in case 2 of parameter variations is approximately 0.0061mm. The maximum parameter variation between the nominal battery and that of case 2 is only 5%. Nonetheless, the variation in the maximum response is almost 30%. This demonstrates that

small local structural variations can have large global consequences. To efficiently capture the dynamic characteristics of the structure with simultaneous pre-stress and structural variations, we developed the new approach described in the next section.

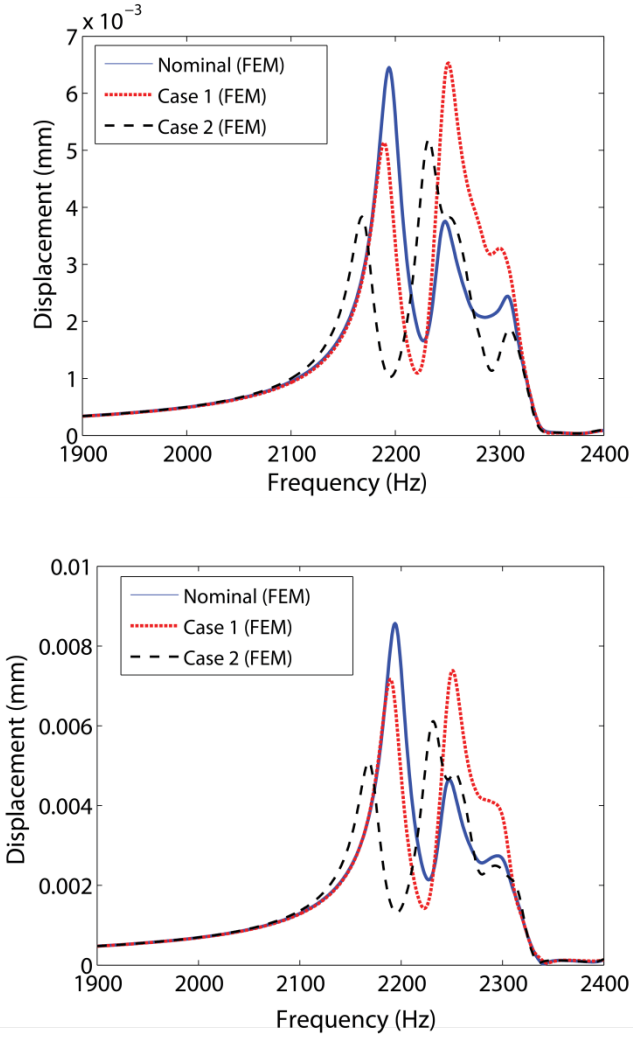

Figure 6. Forced response of the center node of the 4th cell (top) and the 6th cell (bottom) for the nominal case of no parameter variations versus two cases with parameter variations

PARAMETRIC REDUCED-ORDER MODELS

Modeling Pre-stress in a Structure

The pre-stress affects the dynamic response of structures by changing their stiffness. The first key idea of PROMs is the parameterization of the stiffness matrices [14]. The parameterization significantly reduces the reanalysis time because any variation in the parametric range can be applied for different levels of pre-stress without full-order finite element calculations or mesh refinement. The other key idea is to predict vibration responses using reduced-order models (ROMs) as opposed to full-order models to reduce the calculation time. To detail the construction of PROMs, these two key ideas are implemented.

The transformation matrix for PROMs is constructed by a set of fixed-interface normal modes $\mathbf{\Phi}_{aug}^{N}$ given by

$$\mathbf{\Phi}_{aug}^{N} = \left[\mathbf{\Phi}_{0}^{N} \quad \mathbf{\Phi}_{1}^{N} \quad \mathbf{\Phi}_{2}^{N} \quad \mathbf{\Phi}_{3}^{N} \right], \tag{1}$$

where matrix $\mathbf{\Phi}_{0}^{N}$ corresponds to the nominal parameter values and matrices $\mathbf{\Phi}_{i}^{N}\ (i = 1,2,3)$ correspond to 3 other parameter values. A third-order interpolation is used for a parameterization. Thus, 4 samples of matrices (at distinct parameter values) are needed for constructing the transformation matrix.

In general, the columns of $\mathbf{\Phi}_{aug}^{N}$ are not orthogonal. Therefore, for numerical stability, an orthogonal basis for the space spanned by these modes is computed. This basis is obtained by a truncated set of left singular vector $\mathbf{U}^{N}$ of $\mathbf{\Phi}_{aug}^{N}$ [14]. The basis of vectors in $\mathbf{U}^{N}$ is orthogonal, so numerical conditioning problems are avoided. In addition, the left singular vectors $\mathbf{U}^{N}$ are truncated to lower the size of the resulting model. The choice of the cutoff point can affect accuracy if it is chosen too high, but it does not affect numerical stability. Thus, the cutoff value can be estimated by a standard convergence study where calculations are done at ever lower cutoff values until convergence is obtained. For the calculations we performed, the cutoff was 0.01% of the maximum singular value. Then $\mathbf{U}^{N}$ is used in a transformation matrix $\mathbf{T}^{PROM}$ to convert for physical coordinates to generalized coordinates. The transformed stiffness matrices for the 4 samples of such matrices

$$\mathbf{K}_{i}^{PROM} = \left(\mathbf{T}^{PROM}\right)^{T} \mathbf{K}_{i}^{FEM} \mathbf{T}^{PROM}, \tag{2}$$

where $i = 0, 1, 2, 3$.

For convenience we summarize next the parameterization procedure closely following Hong et al. [14]. The parameterization equation consists of a third-order interpolation, which can be written as

$$\mathbf{K}\left(p_0 + \Delta p\right) \approx \mathbf{K}_0 + \Delta p \mathbf{K}_1 + \Delta p^2 \mathbf{K}_2 + \Delta p^3 \mathbf{K}_3 . \tag{3}$$

Four equations are needed to calculate the matrices $\mathbf{K}_i$ (for $i = 0, 1, 2, 3$). To obtain these four equations, reduced-order stiffness matrices are computed using Equation (2) for four parameter values. First, consider the case where $\Delta p = 0$. One obtains

$$\mathbf{K}(p_0) \approx \mathbf{K}_0^{PROM}. \tag{4}$$

Next, consider $\Delta p = i\delta p$ (for $i = 1, 2, 3$). One obtains

$$\begin{aligned}\mathbf{K}(p_0 + i\delta p) &\approx \mathbf{K}_i^{PROM} \\ &\approx \mathbf{K}_0 + (i\delta p)\mathbf{K}_1 + (i\delta p)^2 \mathbf{K}_2 + (i\delta p)^3 \mathbf{K}_3 .\end{aligned} \tag{5}$$

Rearranging Equations (4) and (5) into matrix form, for each entry e, q of the matrices $\mathbf{K}_0$, $\mathbf{K}_1$, $\mathbf{K}_2$ and $\mathbf{K}_3$, one obtains

$$\mathbf{C}\begin{bmatrix}\mathbf{K}_{0,eq} \\ \mathbf{K}_{1,eq} \\ \mathbf{K}_{2,eq} \\ \mathbf{K}_{3,eq}\end{bmatrix} = \begin{bmatrix}\mathbf{K}(p_0)_{eq} \\ \mathbf{K}(p_0 + \delta p)_{eq} \\ \mathbf{K}(p_0 + 2\delta p)_{eq} \\ \mathbf{K}(p_0 + 3\delta p)_{eq}\end{bmatrix}, \tag{6}$$

where

$$\mathbf{C} = \begin{bmatrix}1 & 0 & 0 & 0 \\ 1 & \delta p & (\delta p)^2 & (\delta p)^3 \\ 1 & 2\delta p & (2\delta p)^2 & (2\delta p)^3 \\ 1 & 3\delta p & (3\delta p)^2 & (3\delta p)^3\end{bmatrix}. \tag{7}$$

Equation (6) can be easily solved by simply inverting the 4×4 matrix $\mathbf{C}$. Let us denote by $\mathbf{A}$ this inverse matrix, i.e.

$$\mathbf{A} = \mathbf{C}^{-1} = \begin{bmatrix}\mathbf{A}_{11} & \mathbf{A}_{12} & \mathbf{A}_{13} & \mathbf{A}_{14} \\ \mathbf{A}_{21} & \mathbf{A}_{22} & \mathbf{A}_{23} & \mathbf{A}_{24} \\ \mathbf{A}_{31} & \mathbf{A}_{32} & \mathbf{A}_{33} & \mathbf{A}_{34} \\ \mathbf{A}_{41} & \mathbf{A}_{42} & \mathbf{A}_{43} & \mathbf{A}_{44}\end{bmatrix}. \tag{8}$$

Rearranging Equation (6) using the entries $\mathbf{A}$, one obtains

$$\begin{aligned}\mathbf{K}(p_0 + \Delta p) &\approx \mathbf{K}_{\Delta p}^{PROM} \\ &\approx b_0\mathbf{K}_0^{PROM} + b_1\mathbf{K}_1^{PROM} + b_2\mathbf{K}_2^{PROM} + b_3\mathbf{K}_3^{PROM},\end{aligned} \tag{9}$$

where

$$\begin{aligned}b_0 &= \left(A_{11} + A_{21}\Delta p + A_{31}\Delta p^2 + A_{41}\Delta p^3\right), \\ b_1 &= \left(A_{12} + A_{22}\Delta p + A_{32}\Delta p^2 + A_{42}\Delta p^3\right), \\ b_2 &= \left(A_{13} + A_{23}\Delta p + A_{33}\Delta p^2 + A_{43}\Delta p^3\right), \\ b_3 &= \left(A_{14} + A_{24}\Delta p + A_{34}\Delta p^2 + A_{44}\Delta p^3\right).\end{aligned}$$

The parameterized stiffness matrix in Equation (9) is used to capture the dynamic response of the structure with different levels of pre-stress. Details of this procedure can be found also in Hong et al. [14].

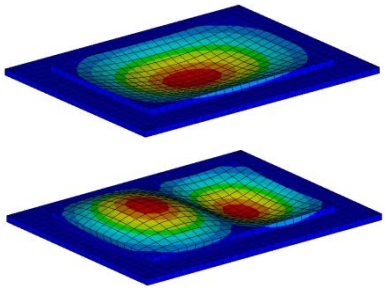

Figure 7. 1st and 2nd modes of a fixed-boundary pouch cell

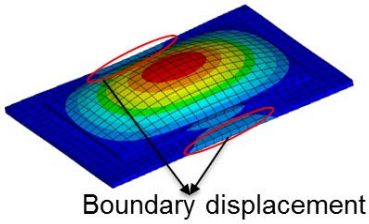

Figure 8. Boundary-displaced motion of a pouch cell

Modeling Structural Variations in Cells

The equations of motion for the structure with no variation and with variation can be expressed as

$$\mathbf{M}\ddot{\mathbf{x}} + \mathbf{C}\dot{\mathbf{x}} + \mathbf{K}\mathbf{x} = \mathbf{F}, \tag{10}$$

$$\mathbf{M}\ddot{\mathbf{x}} + \mathbf{C}\dot{\mathbf{x}} + \left(\mathbf{K} + \mathbf{K}^{\delta}\right)\mathbf{x} = \mathbf{F}, \tag{11}$$

where $\mathbf{K}^{\delta}$ contains the stiffness variation. Based on equations (10) and (11), the mode shapes are defined by the following eigenvalue problems

$$\mathbf{K}\mathbf{\Phi}^t - \mathbf{M}\mathbf{\Phi}^t\mathbf{\Lambda}^t = \mathbf{0}, \tag{12}$$

$$\left(\mathbf{K} + \mathbf{K}^{\delta}\right)\mathbf{\Phi}^m - \mathbf{M}\mathbf{\Phi}^m\mathbf{\Lambda}^m = \mathbf{0}, \tag{13}$$

where superscript t and m indicate the tuned (nominal) and mistuned (structure with variation) quantities. Matrices $\mathbf{\Lambda}^t$ and $\mathbf{\Lambda}^m$ are diagonal and contain the eigenvalues of the tuned and mistuned systems. If the structure has mass variations, the mass matrix in Equation (11) is $\left(\mathbf{M} + \mathbf{M}^{\delta}\right)$. For the sake of simplicity, we consider just the case of stiffness variations.

The novel approach is based on two key assumptions. The first assumption is that the mode shapes $\mathbf{\Phi}^m$ of a pack with

parametric variations can be approximated as a linear combination of the mode shapes $\mathbf{\Phi}^t$ of nominal pack with no parametric variations. This first assumption is ensured by the high modal density.

The second assumption for structural variations is that the variations in stiffness of a cell can be projected onto a small set of modes of the nominal cell with a fixed boundary, as shown in Figure 7. This second assumption relies on the fact that the boundary motions can be ignored when the boundary of the pouch cell is not moving. However, it turns out that the boundary motion has to be considered because it is not small, as shown in Figure 8. Thus, the plate-like modes of a nominal cell—with its boundary displaced the same amount as the frame—are used in the proposed PROMs. This is a key step for ensuring accuracy. This approach is distinct from the original CMM method [15] because the CMM method does not account for the boundary motion.

These two key ideas are implemented to model a system with pre-stress variations. Equation (10) for the tuned (nominal) structure with pre-stress variations can be written as

$$\mathbf{M}_{\Delta p,0}^{PROM}\ddot{\mathbf{u}}^{PROM}+(1+j\gamma)\mathbf{K}_{\Delta p,0}^{PROM}\mathbf{u}^{PROM}=\mathbf{F}^{PROM}, \qquad (14)$$

where $\mathbf{u}^{PROM}$ are generalized coordinates given by $\mathbf{x}=\mathbf{T}^{PROM}\mathbf{u}^{PROM}$. Subscript Δp indicates the pre-stress variation and subscript 0 indicates no structural variations. γ is a structural damping coefficient.

The eigenvalue problem determined from Equation (14) with $\mathbf{F}^{PROM}=\mathbf{0}$ is solved to determine the natural frequencies $\mathbf{\Lambda}_{\Delta p,0}^{PROM}$ and mode shapes $\mathbf{\Phi}_{\Delta p,0}^{PROM}$ of the system. Next, we can use a secondary modal analysis to transform coordinates from $\mathbf{u}^{PROM}$ to $\mathbf{v}^{PROM}$ such that $\mathbf{u}^{PROM}=\mathbf{\Phi}_{\Delta p,0}^{PROM}\mathbf{v}^{PROM}$. Equation (14) becomes

$$\ddot{\mathbf{v}}^{PROM}+(1+j\gamma)\mathbf{\Lambda}_{\Delta p,0}^{PROM}\mathbf{v}^{PROM}=\left(\mathbf{\Phi}_{\Delta p,0}^{PROM}\right)^T\mathbf{F}^{PROM}. \qquad (15)$$

Note that $\mathbf{\Lambda}_{\Delta p,0}^{PROM}$ contains eigenvalues of the pre-stressed structure without variation. That is different from $\mathbf{\Lambda}^t$ which contains eigenvalues of the tuned system without pre-stress.

As described above, the first key assumption is used in the PROM domain. The mistuned mode shapes of the structure can be represented as a linear combination of tuned mode shapes. Thus, we can assume the physical coordinates $\mathbf{x}$ in Equation (11) can be expressed as

$$\mathbf{x}=\mathbf{T}^{PROM}\mathbf{u}^{PROM}=\mathbf{T}^{PROM}\mathbf{\Phi}_{\Delta p,0}^{PROM}\mathbf{v}^{PROM}. \qquad (16)$$

Then the equations of motion of the mistuned structure in the $\mathbf{v}^{PROM}$ coordinates can be written as

$$\ddot{\mathbf{v}}^{PROM}+(1+j\gamma)\left(\mathbf{\Lambda}_{\Delta p,0}^{PROM}\mathbf{v}^{PROM}+\mathbf{A}\right)=\left(\mathbf{\Phi}_{\Delta p,0}^{PROM}\right)^T\mathbf{F}^{PROM}, \qquad (17)$$

where $\mathbf{A}=\left(\mathbf{\Phi}_{\Delta p,0}^{PROM}\right)^T\left(\mathbf{T}^{PROM}\right)^T\mathbf{K}_{\Delta p,\delta}^{FEM}\mathbf{T}^{PROM}\mathbf{\Phi}_{\Delta p,0}^{PROM}\mathbf{v}^{PROM}$ and $\mathbf{K}_{\Delta p,\delta}^{FEM}$ contains the variations in the stiffness matrix in physical coordinates between the nominal structure and the structure with variations.

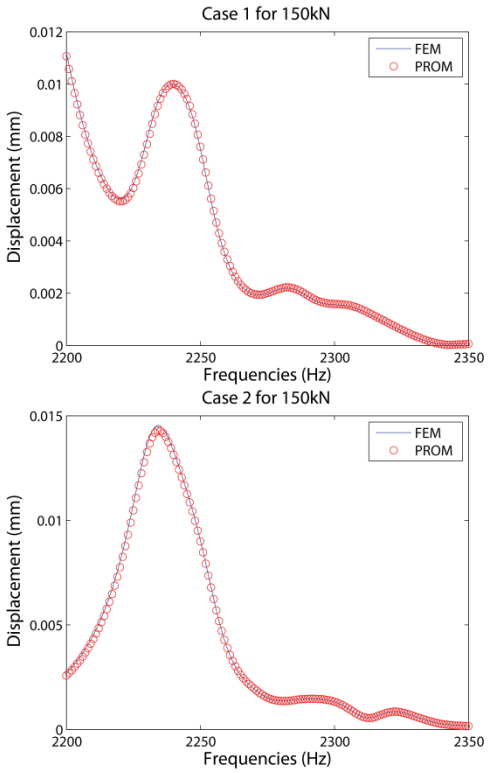

Figure 9. Forced response predictions for the center node of the 5th cell (top) and the 9th cell (bottom) predicted by a full-order model and a PROM for cases 1 (top) and 2 (bottom) with 150kN pre-stress

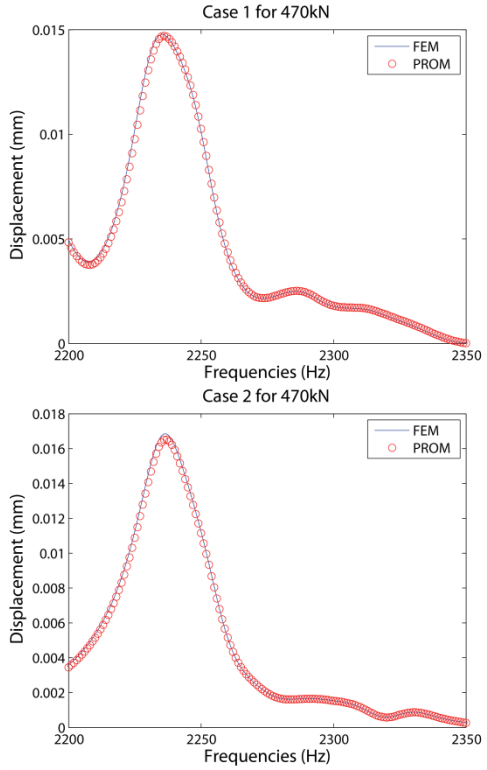

Figure 10. Forced response predictions for the center node of the 5th cell (top) and the 9th cell (bottom) predicted by a full-order model and a PROM for cases 1 (top) and 2 (bottom) with 470kN pre-stress

To parameterize the stiffness variation in the j^{th} cell, we used a first order interpolation given by

$$\mathbf{K}_{\Delta p,\delta}^{FEM,j} = m_j \mathbf{K}_{\Delta p,0}^{FEM,j}, \tag{18}$$

where $\mathbf{K}_{\Delta p,0}^{FEM,j}$ is the j^{th} cell stiffness matrix for the nominal cell, and m_j is the amount of stiffness variation in the j^{th} cell.

Then, $\mathbf{K}_{\Delta p,0}^{FEM,j}$ can be partitioned into

$$\mathbf{K}_{\Delta p,0}^{FEM,j} = \begin{bmatrix} \mathbf{K}_{AA}^0 & \mathbf{K}_{AO}^0 \\ \mathbf{K}_{OA}^0 & \mathbf{K}_{OO}^0 \end{bmatrix}, \tag{19}$$

where subscripts *A* and *O* refer to interface (A) and internal (O) DOFs of the j^{th} cell. The partitions of the stiffness matrix are used to calculate the static deformation from the boundary displacement of the j^{th} cell by using

$$\begin{bmatrix} \mathbf{K}_{AA}^0 & \mathbf{K}_{AO}^0 \\ \mathbf{K}_{OA}^0 & \mathbf{K}_{OO}^0 \end{bmatrix} \begin{bmatrix} \overline{\mathbf{T}}_{A,j} \\ \overline{\mathbf{T}}_{O,j} \end{bmatrix} = \begin{bmatrix} \mathbf{F}_A \\ \mathbf{F}_O \end{bmatrix}, \tag{20}$$

where $\overline{\mathbf{T}}_{A,j}$ and $\overline{\mathbf{T}}_{O,j}$ are interface and internal displacements of the j^{th} cell. The interface displacement $\overline{\mathbf{T}}_{A,j}$ is obtained from the transformation matrix $\mathbf{T}^{PROMs}$ by selecting entries corresponding to interface DOFs of the j^{th} cell from global DOFs, which is

$$\overline{\mathbf{T}}_{A,j} = \mathbf{T}_{A,j}^{PROM}. \tag{21}$$

Then the static deformation induced by the boundary displacement can be computed from Equation (20), that is

$$\overline{\mathbf{T}}_j = \begin{bmatrix} \overline{\mathbf{T}}_{A,j} \\ \overline{\mathbf{T}}_{O,j} \end{bmatrix} = \begin{bmatrix} \mathbf{T}_{A,j}^{PROM} \\ -\left(\mathbf{K}_{OO}^0\right)^{-1} \mathbf{K}_{OA}^0 \mathbf{T}_{A,j}^{PROM} \end{bmatrix}. \tag{22}$$

Next, a set of fixed interface normal modes $\mathbf{\Phi}^C$ of a single battery cell structure are calculated. The fixed-interface normal modes are a truncated set of modes obtained by solving the eigenproblem with the mass and stiffness matrices of the cell with a fixed boundary. One obtains

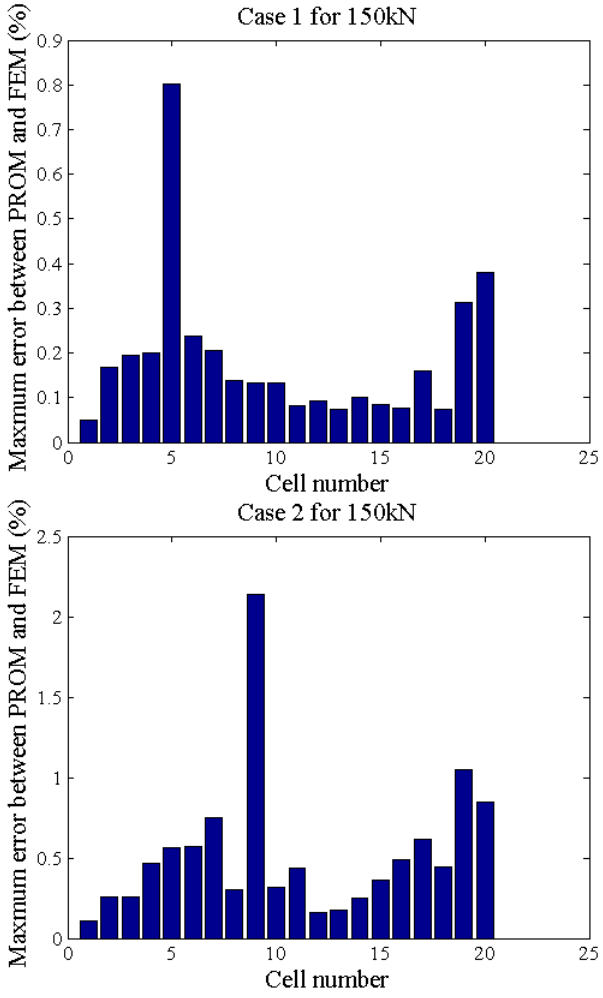

Figure 11. Maximum errors between PROM and FEM for each cell (center node displacement) in the frequency range of interest for cases 1 (top) and 2 (bottom) with 150kN pre-stress

$$\mathbf{K}_{OO}^{0}\boldsymbol{\Phi}_{OO}^{C}-\mathbf{M}_{OO}^{0}\boldsymbol{\Phi}_{OO}^{C}\boldsymbol{\Lambda}^{C}=\mathbf{0}\,, \tag{23}$$

where $\boldsymbol{\Phi}^{C}=\begin{bmatrix}\boldsymbol{\Phi}_{AA}^{C}\\ \boldsymbol{\Phi}_{OO}^{C}\end{bmatrix}=\begin{bmatrix}\mathbf{0}\\ \boldsymbol{\Phi}_{OO}^{C}\end{bmatrix}$.

Next, the computed static deformation $\overline{\mathbf{T}}_j$ and a set of fixed interface normal modes $\boldsymbol{\Phi}^{C}$ of the single cell are used to calculate modal participation factors $\mathbf{q}_j$ as follows

$$\begin{aligned}&\mathbf{T}_j^{PROM}-\overline{\mathbf{T}}_j=\boldsymbol{\Phi}^{C}\mathbf{q}_j\,,\\ &\mathbf{q}_j=\left(\boldsymbol{\Lambda}^{C}\right)^{-1}\left(\boldsymbol{\Phi}^{C}\right)^{T}\mathbf{K}_{\Delta p,\delta}^{FEM,j}\left(\mathbf{T}_j^{PROM}-\overline{\mathbf{T}}_j\right).\end{aligned} \tag{24}$$

These relations are used to construct the equations of motion for pre-stress and stiffness variations as follows

$$\ddot{\mathbf{v}}^{PROM}+(1+j\gamma)\boldsymbol{\Lambda}_{\Delta p,0}^{PROM}\mathbf{v}^{PROM}+\mathbf{B}=\left(\boldsymbol{\Phi}_{\Delta p,0}^{PROM}\right)^{T}\mathbf{F}^{PROM}\,, \tag{25}$$

where

$\mathbf{B}=(1+j\gamma)\left(\boldsymbol{\Phi}_{\Delta p,0}^{PROM}\right)^{T}\mathbf{C}\boldsymbol{\Phi}_{\Delta p,0}^{PROM}\mathbf{v}^{PROM}$,

$\mathbf{C}=\left[\sum_{j=1}^{N}\left(\boldsymbol{\Phi}^{C}\mathbf{q}_j+\overline{\mathbf{T}}_j\right)^{T}m_j\mathbf{K}_{\Delta p,0}^{FEM,j}\left(\boldsymbol{\Phi}^{C}\mathbf{q}_j+\overline{\mathbf{T}}_j\right)\right]$, and N is the number of cells which have stiffness variations.

NUMERICAL RESULTS

Numerical results to demonstrate the performance of the proposed method have been obtained using the academic battery model shown in Figure 1. This academic model has 208,753 DOFs and 20 nominally identical cells. The frequency range of interest is 1,500 – 3,000Hz (the first flat region in Figure 4). Pre-stress and dynamic loads were applied as shown in Figure 1. Two cases of Young's modulus variations were applied to 4 cells in the pack under the pre-stress of 150kN and 470kN, as shown in Table 1. The forced response is obtained at the center nodes of all 20 cells.

The PROM predictions agree very well with the FEM results. For example, Figures 9 and 10 show the response of the center node of the 5th cell for case 1 and the 9th cell for case 2 under 150kN and 470kN pre-stress, respectively. The solid lines indicate predictions of full-order models and the symbols indicate PROM predictions. Figures 11 and 12 show the maximum error between the PROM and the FEM predictions for all cells over the entire frequency range of interest for cases 1 and 2 under different levels of pre-stress. The maximum errors are not larger than 2.7% as shown in Figures 11 and 12. In Table 2, the number of DOFs and the computational time required for the reanalyses are shown. The number of DOFs of the PROM is much lower than that of the full-order finite element model (which has 208,753 DOFs). The reanalysis time required by the PROM for each variation is about 10,000 times shorter than that of the full-order models.

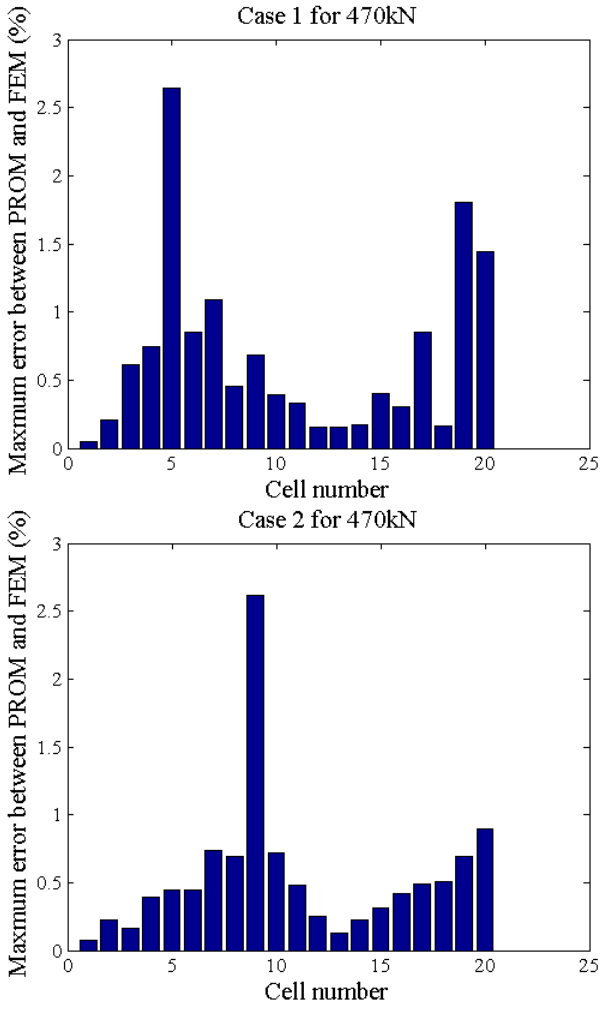

Figure 12. Maximum errors between PROM and FEM for each cell (center node displacement) in the frequency range of interest for cases 1 (top) and 2 (bottom) with 470kN pre-stress

This computational gain is expected to be even larger for more refined models. That is because the PROM captures the low-dimensional physics of the problem. This low dimensionality means that only a few coordinates are necessary to describe the dynamics of the actual physical system. This number of coordinates is a feature of the physics, not of the model used to discretize the physics. The model can increase in size by mesh refinement. However, the physics remains the same and require only a few coordinates. The key is to find these coordinates, and PROM techniques are intended to do just that. Thus, the size of the PROM is not expected to increase when the size of the full order model increases (e.g., by mesh refinement).

In a battery pack, a single pouch cell with intense vibrations may lead to the failure of the entire pack. Thus, identifying the cell that is most likely to have intense vibrations is a key issue. The accuracy and high computational speed of the PROMs

allow a very rapid identification of the cells most influenced by parameter variations (pre-stress and structural variations).

Table 2. Comparison of the full-order model and the PROM

	Full-order model	PROM
System DOFs	208,753	38
Reanalysis time	10,120-10,780 sec	0.89-0.95

For that, the forced response is collected for all cells. A cell amplification factor (CAF) is defined as

$$CAF^{\,j} = \max_{i=1,\cdots,N}\left(\frac{\max_{\omega}\left|A_i^{\Delta p}\right|}{\max_{\omega}\left|A_i^{\text{nominal}}\right|}\right), \qquad (26)$$

where ω is the frequency of the excitation, $A_i^{\Delta p}$ is the amplitude of the response of cell *i* of a battery with parameter variations, and A_i^{nominal} is the amplitude of the response of cell *i* of the battery with nominal parameters. Intense vibrations occur in the cell with the largest cell amplification factor in the system. The superscript *j* is the case of variation, and *N* indicates the number of cells. As shown in Figures 9 and 10, the forced response is significantly different for each case of variation. That means that the cell being the worst should be detected by a statistical analysis. Herein, cell amplification factors were calculated for 10,000 cases of random cell-to-cell variations for two-levels of pre-stress with 150kN and 470kN as shown in Figure 13. Figure 14 shows the probability of cell with intense vibrations for these two pre-stresses. These results highlight that the 1st cell suffers the largest amplification due to random variations and pre-stress. For example, the largest amplification factor was 3.5 and 3.9 on the 1st cell for 150kN and 470kN respectively. This means that at least one cell had a forced response that was 350% or 390% higher than would be predicted if all the cells were assumed to be identical.

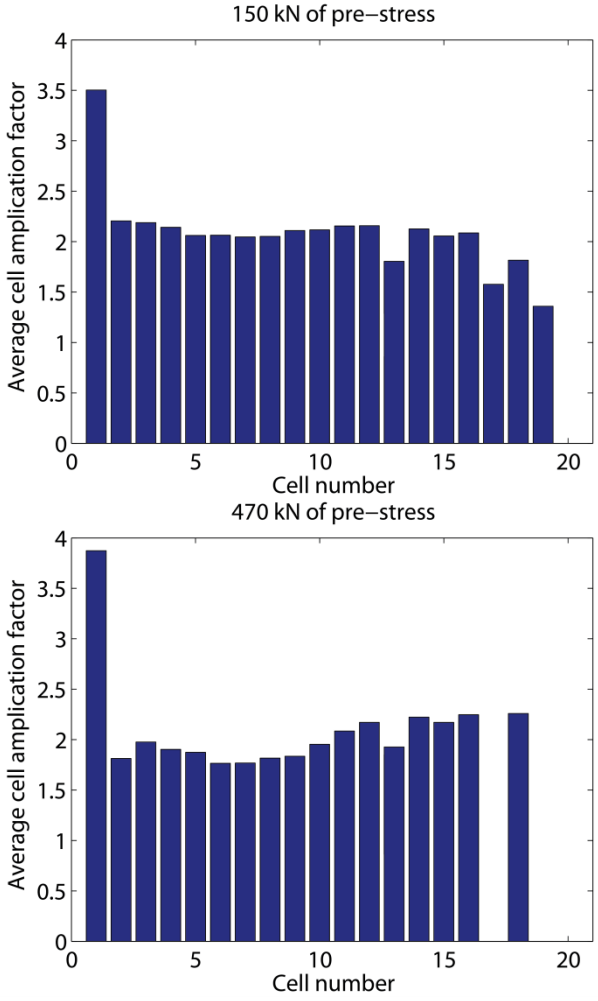

Figure 13. Average cell amplification factors based on 10,000 separate cases of random variations with 150kN (top) and 470kN (bottom) of pre-stress

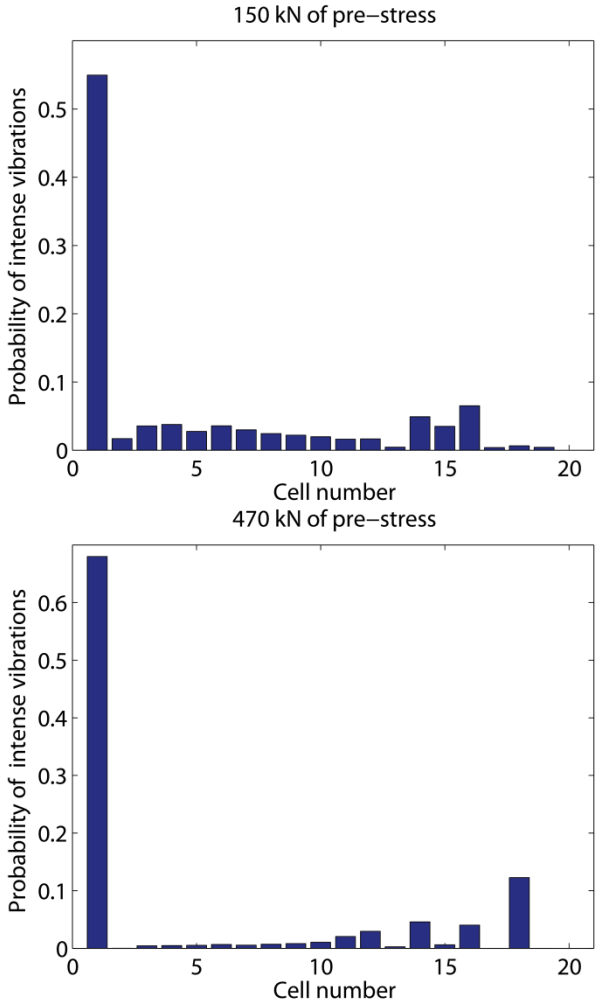

Figure 14. Probability of intense vibrations for each cell based on 10,000 separate cases of random variations with 150kN (top) and 470kN (bottom) pre-stress

When considering random parametric variations in the cells, the worst case of vibrations occurs when the amplification is the largest. This worst case is important because it can be used as a predictor of whether the battery pack may suffer from high local stresses. Results obtained for the maximum cell amplification factor of each cell are shown in Figure 15. Note that the maximum CAF is much greater for cell 1 than for any other cell. This is because the forcing was applied at the end of the battery pack where cell 1 is located. As noted earlier, the parametric variations cause spatial localization of the vibration modes. The modes localized about cell 1 will tend to be strongly excited by the forcing. This confinement of vibration energy is a well known characteristic of nominally periodic structures with small, random parametric variations [18].

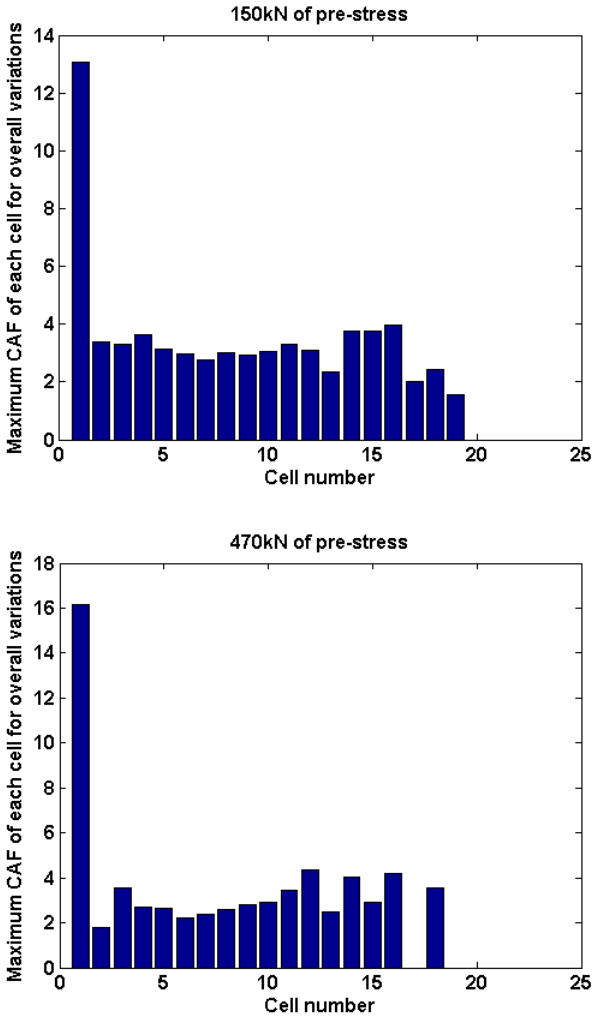

Figure 15. Maximum cell amplification factors for each cell (for overall cases of random variations) with 150kN (top) and 470kN (bottom) pre-stress

For the two cases of pre-stress, namely 150kN and 470kN, the maximum cell amplification factor for the 1st cell is 12.5 and 16.1 respectively. This level of forced response increase could potentially lead to a significant reduction in battery fatigue life. Therefore, these results suggest that it may be important to account for parameter variations in the cells when predicting the structural response and fatigue life of HEV batteries.

CONCLUSIONS

There is currently a lot of research interest in various aspects of hybrid electric vehicle (HEV) battery performance. The scope of this paper is the structural and dynamic characteristics of HEV battery packs. The dynamic characteristics of HEV battery packs are significantly affected by the pre-stress created by joining cells within the pack. Also the dynamic response of the structure can be sensitive to small structural variations among the battery cells because the system features high modal density. Thus, to predict the fatigue life, statistical calculations should be performed. However, a structural finite element model of a full HEV battery could easily have millions of degrees of freedom. The large model size makes it cumbersome or infeasible to run Monte-Carlo-type simulations.

In this paper, we developed new parametric reduced-order models (PROMs) to predict very quickly the structural dynamic response of HEV batteries. We applied the idea of the next generation parametric reduced-order models to capture the different levels of pre-stress using a numerically stable transformation matrix and a third-order interpolation function. Also, to capture the cell-to-cell variation in the entire battery pack, new PROMs are used, which are based on two key assumptions: (1) mode shapes of the structure with variations can be represented as a linear combination of mode shapes of the structure with nominal parameters, and (2) variability in parameters in the corresponding cell can be captured by mode shapes of the nominal cell with its boundary displaced the same amount as the frame.

As a numerical example, a PROM was generated for an academic model of a battery pack with 20 pouch cells. The forced response results from the PROM were found to match very well with those from the full-order finite element model. The results also showed that pre-stress and small local variations in the structural parameters of the cells induce very large changes in the global response.

To help predict which cell is most likely to suffer fatigue failure, we defined an amplification factor that corresponds to the ratio of maximum forced response levels for the system with and without parameter variations. For the 10,000 cases of random variations considered, the largest amplification factor was around 3.5 and 3.9 for 150kN and 470kN. Thus, at least one cell had an increase in the forced response level of approximately 350% and 390% when small variations were accounted for (compared to the nominal system in which all cells are assumed to be identical). For the academic battery pack, the 1st cell was identified as the worst. The dynamics of the pack is susceptible to large amplification in frequency ranges where there is a high modal density. These frequency ranges are due to the physics of the pack, not due to the

models. If the pack is subjected to external loads which contain frequencies in one of these ranges, large vibration and stress amplifications can occur. These observations for pouch cells should also hold for solid prismatic cells. Cylindrical type cells may exhibit a different behavior.

REFERENCES

1. W. C. Hurty, "Dynamic analysis of structural systems using component modes", *AIAA Journal*, Vol. 3, No. 4, pp. 678–685, 1965.
2. R. R. Craig, Jr., M. C. C. Bampton, "Coupling of substructures for dynamic analyses", *AIAA Journal*, Vol. 6, No. 7, pp. 1313–1319, 1968.
3. S. Rubin, "Improved component-mode representation for structural dynamic analysis", *AIAA Journal*, Vol. 13, No. 8, pp. 995–1006, 1975.
4. R. M. Hintz, "Analytical methods in component mode synthesis", *AIAA Journal*, Vol. 13, No. 8, pp. 1007–1016, 1975.
5. R. R. Craig, Jr., C.-J. Chang, "Free-interface methods of substructure coupling for dynamic analysis", *AIAA Journal*, Vol. 14, No. 11, pp. 1633–1635, 1976.
6. M. P. Castanier, Y.-C. Tan, C. Pierre, "Characteristic constraint modes for component mode synthesis", *AIAA Journal*, Vol. 39, No. 6, pp. 1182–1187, 2001.
7. W.-H. Shyu, J. Gu, G. M. Hulbert, Z.-D. Ma, "On the use of multiple quasistatic mode compensation sets for component mode synthesis of complex structures", *Finite Elements in Analysis and Design*, Vol. 35, No. 2, pp. 119–140, 2000.
8. E. Balmès, "Parametric families of reduced finite element modes: Theory and application", *Mechanical Systems and Signal Processing*, Vol. 10, No. 4, pp. 381–394, 1996.
9. E. Balmès, F. Ravary, D. Langlais, "Uncertainty propagation in modal analysis", *in Proceedings of IMAC-XXII: A Conference and Exposition on Structural Dynamics*, Dearborn, MI, pp. IMAC–XXII–57, 2004.
10. G. Zhang, M. P. Castanier, C. Pierre, "Integration of component-based and parametric reduced-order modeling methods for probabilistic vibration analysis and design", *in Proceedings of the Sixth European Conference on Structural Dynamics*, Paris, France, pp. 993–998, 2005.
11. K. Park, G. Zhang, M. P. Castanier, C. Pierre, "A component-based parametric reduced-order modeling technique and its application to probabilistic vibration analysis and design optimization", *in Proceedings of ASME International Mechanical Engineering Congress and Exposition*, Chicago, IL, USA, pp. IMECE2006–15069, 2006.
12. K. Park, "Component-based vibration modeling methods for fast reanalyses and design of complex structures", Ph.D. thesis, University of Michigan, 2008.
13. S. K. Hong, B. I. Epureanu, M. P. Castanier, D. J. Gorsich, "Parametric reduced-order models for predicting the vibration response of complex structures with component damage and uncertainties", *Journal of Sound and Vibration*, Vol. 330, pp. 1091–1110, 2011.
14. S. K. Hong, B. I. Epureanu, M. P. Castanier, "Next-Generation Parametric reduced-order models", *Mechanical Systems and Signal Processing*, DOI 10.1016/j.ymssp.2012.12.012, 2012.
15. S.-H Lim, R. Bladh, and M. P. Castanier, "Compact, generalized component mode mistuning representation for modeling bladed disk vibration", *AIAA Journal*, Vol. 45, No. 9, pp. 2285-2298, 2007.
16. M.-T. Yang, J.H. Griffin, "A reduced-order model of mistuning using a subset of nominal system modes", *Journal of Engineering for Gas Turbines and Power* , Vol. 123, No. 4, pp. 893-900, 2001.
17. S.-H. Lim, C. Pierre, M.P. Castanier, "Predicting blade stress levels directly from reduced-order vibration models of mistuned bladed disks", *Journal of Turbomachinery* , Vol. 128, pp. 206-210, 2006.
18. C. H. Hodges, "Confinement of Vibration by Structural Irregularity," *Journal of Sound and Vibration*, Vol. 82, No. 3, pp. 411-424, 1982.

ACKNOWLEDGMENTS

Funding for this work was provided in part by the Automotive Research Center (ARC), a US Army center of excellence for modeling and simulation of ground vehicles. Funding for the work of the third author was provided in part by the Chief Scientist's Office of the US Army Tank Automotive Research, Development, and Engineering Center (TARDEC) under a mobility research program. Any opinions, findings, conclusions, or recommendations expressed in this material are those of the authors and do not necessarily reflect the views of the US Army.